Available online at www.sciencedirect.com

SciVerse ScienceDirect

Solar Energy 86 (2012) 1222–1231

SOLAR ENERGY

www.elsevier.com/locate/solener

A new dynamic test method for thermal performance of all-glass evacuated solar air collectors

Li Xu [a,b], Zhifeng Wang [a,*], Guofeng Yuan [a], Xing Li [c], Yi Ruan [c]

[a] Key Laboratory of Solar Thermal Energy and Photovoltaic System of Chinese Academy of Sciences, Institute of Electrical Engineering, Beijing 100190, China

[b] Graduate University of the Chinese Academy of Sciences, Beijing 100049, China

[c] Himin Solar Energy Group Co., Ltd., Shandong 253000, China

Received 23 June 2011; received in revised form 14 November 2011; accepted 19 January 2012
Available online 28 February 2012

Communicated by: Associate Editor Bibek Bandyopadhyay

Abstract

A new study on testing thermal performance of all-glass evacuated solar collectors with the air as heat transfer fluid under dynamic conditions outdoors has been developed. The model of this dynamic method was established with the energy balance analysis on solar collectors of this type. Compared with the first order model under steady-state conditions, this model can characterize thermal efficiency of solar collectors under more extensive conditions, reducing considerable operating time spent in waiting for the right test conditions. Through the derivation of the proposed model, it proved a strong relationship existed between this model and the first order model mentioned above. The dynamic model projection for the outlet temperatures was in good agreement with the measured result.

Keywords: Solar air collector; Thermal performance; All-glass evacuated tube; Dynamic method

1. Introduction

A reliable and quick method to test thermal performance of solar collectors outdoors is needed by both solar collector manufacturer and customer while the conventional steady state tests in standards such as the ASHRAE 93-2003 (ASHRAE, 2003), EN 12579-2 (EN, 2006) and ISO 9806-1 (ISO, 1994) commonly cost considerable time in terms of rigorous operational requirement, especially for the test spots under unfavorable weather conditions. Several dynamic and quasi-dynamic methods have been provided to transcend limitations of steady state method. One paper (Fischer et al., 2004) presents an improved approach to outdoor performance testing of solar liquid collectors under quasi-dynamic test conditions based on EN 12975-2 and compares three parameter identification tools for it; A new procedure for testing solar flat plate collectors under unsteady weather conditions is developed and compared with steady state ASHRAE 93 (Amer et al., 1999); Nine dynamic test methods for solar flat plate collectors are reviewed and compared based on both theoretical and experimental evaluation (Nayak and Amer, 2000); The paper (Hou et al., 2005) provides a new method for measurement of solar collector time constant without adjusting the inlet temperature to be equal to the ambient temperature needed in ISO 9806-1; The uncertainties of the least square and the weighted least square regression methods in the quasi-dynamic according to EN 12975-2 are calculated and validated (Kratzenberg et al., 2006).

However, these methods are based on flat-plate solar collector, while in China the tests for all-glass evacuated solar collectors become more significant in view of the data that the production of all-glass evacuated tubes was estimated

* Corresponding author. Tel.: +86 10 62520684; fax: +86 10 62587946.
E-mail address: zhifeng@vip.sina.com (Z. Wang).

0038-092X/$ - see front matter © 2012 Elsevier Ltd. All rights reserved.
doi:10.1016/j.solener.2012.01.015

Nomenclature

a_1	algebraic constant, with reference to T^* (W/(m^2 K))
A	algebraic constant, with reference to $dT_{fo}/d\tau$ (1/s))
A_a	aperture area (m^2)
A_{am}	heat loss area from glass tubes to the ambient (m^2)
A_b	effective aperture area for beam radiation (m^2)
A_d	effective aperture area for diffuse irradiation (m^2)
A_f	heat loss area from glass tubes to the fluid (m^2)
B	algebraic constant, with reference to T_{fo} (K/s)
c_b	specific heat capacity of the glass (J/(kg K))
c_f	specific heat capacity of the air (J/(kg K))
C	algebraic constant, with reference to d $T_{fi}/d\tau$ (1/s)
C_b	thermal capacity of glass tubes (J/K)
C_f	thermal capacity of the air in glass tubes (J/K)
D	algebraic constant, with reference to T_{fi} (K/s)
E	algebraic constant, with reference to G (J s/(K m2))
E_b	algebraic constant, with reference to G_b (J s/(K m^2))
E_d	algebraic constant, with reference to G_d (J s/(K m^2))
F	algebraic constant (K/s)
F_R	collector heat removal factor (–)
G	global solar irradiance (W/m^2)
G_b	beam irradiance (W/m^2)
G_d	diffuse solar irradiance (W/m^2)
$K_{\theta b}(\theta)$	incident angle modifier for beam radiation (–)
$K_{\theta d}$	incident angle modifier for diffuse radiation (–)
m_b	mass of glass (kg)
m_f	mass of air in the tube (kg)
$\dot{m}$	mass flow rate of air (kg/s)
R_{bf}	overall heat transfer resistance from glass tubes to the fluid (K/W)
R_{ba}	overall heat transfer resistance from glass tubes to the ambient (K/W)
T_a	ambient temperature (K)
T_b	glass tube temperature (K)
T_f	air temperature in the tube (K)
T_{fo}	collector outlet temperature (K)
$T_{fo,initial}$	temperature leaving collector at the beginning of time constant test period (K)
$T_{fo,t}$	temperature of the heat transfer fluid leaving collector at a specified time (K)
T_{fi}	collector inlet temperature (K)
T^*	reduced temperature difference (m^2 K/W)
U	overall heat loss coefficient of collector with reference to T^* and A_a (W/(m^2 K))
U_{bf}	overall heat loss coefficient from glass tubes to the fluid (W/(m^2 K))
U_{ba}	overall heat loss coefficient from glass tubes to the ambient (W/(m^2 K))
η	collector thermal efficiency (–)
η_0	eta zero (η at $T^* = 0$) (–)
τ	time (s)
$(\tau\alpha)_{en}$	effective transmittance–absorptance product at normal incidence (–)

to be more than 350 million tubes and this type solar collector took an 95% share of the market in 2009 (Tang et al., 2011). Consequently, the efforts to make researches on all-glass evacuated solar collectors have been devoted in recent years. For example, a simulation model and the transverse incidence angle modifier of the water-in-glass solar water heater are presented (Budihardjo and Morrison, 2009); The comparative tests between flat plate and evacuated tube solar collectors in stationary standard EN 12975-2 show that only at low inlet temperature the output energy of the flat plate collector overcomes the one of evacuated tube collector (Zambolin and Del Col, 2010); The thermal performance analysis on one single evacuated tube shows the surface temperature of the absorbing coating is an important parameter (Ma et al., 2010).

For the areas where the solar irradiance is relatively poor quality, the stringent requirements for solar source beyond manual control make the days in a year reduced enormously for the reason that the thermal efficiency test, more often than not, is interrupted. The aim of this study is to solve the problems caused by rigorous conditions for testing the all-glass evacuated solar collectors in the steady state method. Therefore, this dynamic method for testing thermal efficiency of evacuated solar collectors outdoors is supposed to enlarge the test days in the whole year by extending the range of solar irradiation limits.

Through the analysis on energy balance of all-glass evacuated solar air collector, this new dynamic method is proposed to effectively solve the difficulties brought about by severe operational limits for steady state test conditions outdoors, particularly due to uncontrollable weather conditions. For example, during one test period, the global solar irradiance is less than 790 W/m^2 or varies more than $\pm$32 W/m^2, or the diffuse solar irradiance is greater than 20% of global solar irradiance. In these cases, the proposed dynamic method fills the role of characterizing thermal performance of solar collectors while the ASHRAE 93-2003 does not work anymore, which saves actually operational time strikingly rather than expect the perfect weather.

Multiple linear regression (MLR) as the ordinary and convenient math tool to identify parameters is applied to the proposed dynamic model. Once these parameters for

one type of solar air collector are obtained from the common computer software of MLR, they can always be employed to describe thermal performance of this type under different test conditions. Additionally, the time constant can be found in the predicted results obviously on account of the intrinsic thermal capability of a solar collector, which means that the instantaneous change or shock in operational conditions cannot take place in outlet temperature immediately.

2. Mathematical model

Before the establishment of mathematical model, the following general assumptions will be made in the process of the energy balance analysis according to the heat transfer characteristics and the structural features of the all-glass evacuated solar air collector as shown in Fig. 1:

1. The tube-connection box of a solar collector is provided with excellent insulation against its heat loss to the surroundings.
2. The heat accumulation of inner aluminum tubes is ignored.
3. The heat transfer processes among the different components of a solar collector are one dimensional.
4. The mass flowrate of the air through the collector shall be standardized at one value within the variation of ±2% for all data points.
5. During the test process, the incident angle shall be in the near-normal incident range in which the incident angle modifier varies by no more than ±2% from its value at normal incidence by adjusting the rotating racket.

2.1. New dynamic model

Fig. 2 describes the input solar energy and output energy of one all-glass evacuated tube. In the new dynamic model, the global solar irradiance is separated into beam and diffuse portions in order to distinguish their influences on thermal performance of solar collectors. Additionally, the inner glass tube is assumed to own uniform temperature

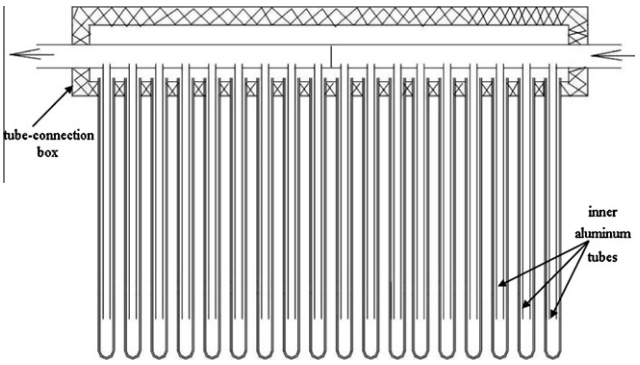

Fig. 1. Schematic of all-glass evacuated solar air collector.

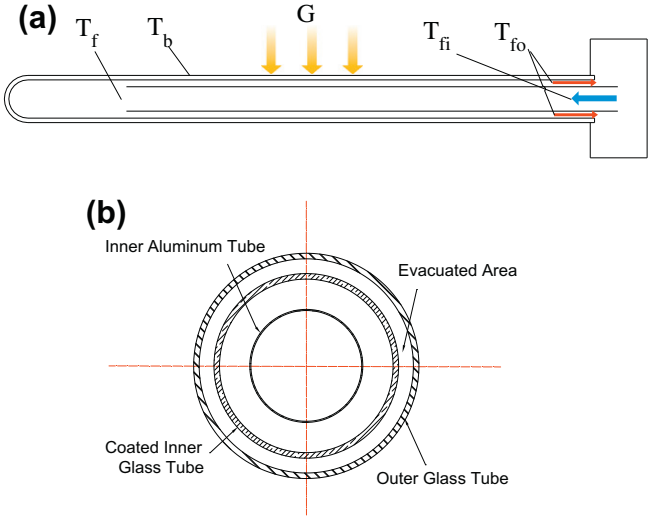

Fig. 2. All-glass evacuated solar air collector tube (a) schematic of one evacuated tube (b) cross section of the tube.

T_b. Thus, the energy balance equation for this glass tube is expressed as

$$m_b c_b \frac{dT_b}{d\tau} = F_R(\iota\alpha)_{en} K_{\theta b}(\theta) A_a G_b + F_R(\iota\alpha)_{en} K_{\theta d} A_a G_d - A_f U_{bf}(T_b - T_f) - A_{am} U_{ba}(T_b - T_a). \quad (1)$$

For the last term, the heat loss also includes the one from the outer glass tube to the ambient by converting it into this form according to the relationship between outer and inner glass tube temperature (Liang et al., 2011), therefore, the U_{ba} is a coupled over heat loss coefficient.

Similarly, when the air in the glass tube is assumed to own uniform temperature T_f, the energy balance equation for the air in glass tubes is expressed as

$$m_f c_f \frac{dT_f}{d\tau} = A_f U_{bf}(T_b - T_f) - \dot{m} c_f (T_{fo} - T_{fi}). \quad (2)$$

According to the fifth assumption, $K_{\theta b}(\theta)$ and $K_{\theta d}$ become constant. As a consequence, by defining $F_R(\iota\alpha)_{en} K_{\theta b}(\theta) A_a = A_b$ and $F_R(\iota\alpha)_{en} K_{\theta d} A_a = A_d$, and using the thermal resistance R_{bf} and R_{ba}, Eqs. (1) and (2) are treated to be simple mathematical expressions shown in Eqs. (3) and (4), respectively.

$$C_b \frac{dT_b}{d\tau} = A_b G_b + A_d G_d - \frac{T_b - T_f}{R_{bf}} - \frac{T_b - T_a}{R_{ba}} \quad (3)$$

$$C_f \frac{dT_f}{d\tau} = \frac{T_b - T_f}{R_{bf}} - \dot{m} c_f (T_{fo} - T_{fi}) \quad (4)$$

Then, Eq. (4) is rearranged as

$$\frac{T_b}{R_{bf}} = C_f \frac{dT_f}{d\tau} + \frac{T_f}{R_{bf}} + \dot{m} c_f (T_{fo} - T_{fi}). \quad (5)$$

Furthermore, Eq. (5) is differentiated with respect to τ.

$$\frac{1}{R_{bf}} \frac{dT_b}{d\tau} = C_f \frac{d^2 T_f}{d\tau^2} + \frac{1}{R_{bf}} \frac{dT_f}{d\tau} + \dot{m} c_f \left(\frac{dT_{fo}}{d\tau} - \frac{dT_{fi}}{d\tau} \right) \quad (6)$$

For the purpose of eliminating T_b in Eq. (3), Eqs. (5) and (6) are employed. Thus, the final combining expression of the two energy balance equations is

$$C_bC_f\frac{d^2T_f}{d\tau^2}+\frac{C_bR_{ba}+C_fR_{ba}+C_fR_{bf}}{R_{bf}R_{ba}}\frac{dT_f}{d\tau}+\frac{T_f}{R_{bf}R_{ba}}=\frac{A_bG_b+A_dG_d}{R_{bf}}-\frac{R_{ba}+R_{bf}}{R_{bf}R_{ba}}\dot{m}c_f(T_{fo}-T_{fi})-C_b\dot{m}c_f\left(\frac{dT_{fo}}{d\tau}-\frac{dT_{fi}}{d\tau}\right)+\frac{T_a}{R_{bf}R_{ba}}. \tag{7}$$

When the outlet temperature T_{fo} is selected as the characteristic temperature of the air in the tube (Hou, 2005), Eq. (7) is changed into

$$\begin{aligned}\frac{1+(R_{bf}+R_{ba})\dot{m}c_f}{C_bC_fR_{bf}R_{ba}}T_{fo}=&-\frac{d^2T_{fo}}{d\tau^2}-\left(\frac{1+\dot{m}c_fR_{bf}}{C_fR_{bf}}+\frac{R_{bf}+R_{ba}}{C_bR_{bf}R_{ba}}\right)\frac{dT_{fo}}{d\tau}+\frac{\dot{m}c_f}{C_f}\frac{dT_{fi}}{d\tau}\\&+\frac{(R_{bf}+R_{ba})\dot{m}c_f}{C_bC_fR_{bf}R_{ba}}T_{fi}+\frac{1}{C_bC_fR_{bf}R_{ba}}T_a+\frac{A_b}{C_bC_fR_{bf}}G_b+\frac{A_d}{C_bC_fR_{bf}}G_d.\end{aligned} \tag{8}$$

As a consequence, the linear differential equation is

$$\frac{d^2T_{fo}}{d\tau^2}+A\frac{dT_{fo}}{d\tau}+BT_{fo}=C\frac{dT_{fi}}{d\tau}+DT_{fi}+E_bG_b+E_dG_d+FT_a. \tag{9}$$

Derived from Eq. (8), the coefficients are expressed in the following equations.

$$A=\frac{1+\dot{m}c_fR_{bf}}{C_fR_{bf}}+\frac{R_{bf}+R_{ba}}{C_bR_{bf}R_{ba}} \tag{10}$$

$$B=\frac{1+(R_{bf}+R_{ba})\dot{m}c_f}{C_bC_fR_{bf}R_{ba}} \tag{11}$$

$$C=\frac{\dot{m}c_f}{C_f} \tag{12}$$

$$D=\frac{(R_{bf}+R_{ba})\dot{m}c_f}{C_bC_fR_{bf}R_{ba}} \tag{13}$$

$$E_b=\frac{A_b}{C_bC_fR_{bf}} \tag{14}$$

$$E_d=\frac{A_d}{C_bC_fR_{bf}} \tag{15}$$

$$F=\frac{1}{C_bC_fR_{bf}R_{ba}} \tag{16}$$

Obviously, $D=B-F$ hence Eq. (9) is rearranged.

$$\frac{d^2T_{fo}}{d\tau^2}+A\frac{dT_{fo}}{d\tau}+B(T_{fo}-T_{fi})=C\frac{dT_{fi}}{d\tau}+E_bG_b+E_dG_d-F(T_{fi}-T_a) \tag{17}$$

Eq. (17) is the basic dynamic mathematical model with the parameters A, B, C, E_b, E_d and F, describing the thermal characteristics of the solar air collector, needed to be identified with the experimental data.

2.2. Deduction of new model

The terms in Eq. (17), $T_{fo}-T_{fi}$ and $T_{fi}-T_a$, indicate that the new dynamic model has a special relationship with the first order model recognized in steady state test for the thermal performance. Accordingly, the expression of Eq. (17) is rearranged again.

$$B(T_{fo}-T_{fi})=-\frac{d^2T_{fo}}{d\tau^2}-A\frac{dT_{fo}}{d\tau}+C\frac{dT_{fi}}{d\tau}+E_bG_b+E_dG_d-F(T_{fi}-T_a) \tag{18}$$

Mathematically, multiplying both sides of Eq. (18) by the term $\frac{\dot{m}c_f}{BGA_a}$ yields

$$\frac{\dot{m}c_f}{GA_a}(T_{fo}-T_{fi})=-\frac{\dot{m}c_f}{BGA_a}\left(\frac{d^2T_{fo}}{d\tau^2}+A\frac{dT_{fo}}{d\tau}-C\frac{dT_{fi}}{d\tau}\right)+\frac{\dot{m}c_f}{BGA_a}(E_bG_b+E_dG_d)-\frac{\dot{m}c_f}{BGA_a}F(T_{fi}-T_a). \tag{19}$$

In order to compare with the first order model in standards mentioned above, the global solar irradiance substitutes for beam irradiance and diffuse solar irradiance.

$$\frac{\dot{m}c_f}{GA_a}(T_{fo}-T_{fi})=-\frac{\dot{m}c_f}{BGA_a}\left(\frac{d^2T_{fo}}{d\tau^2}+A\frac{dT_{fo}}{d\tau}-C\frac{dT_{fi}}{d\tau}\right)+\frac{E\dot{m}c_f}{BA_a}-\frac{F\dot{m}c_f}{BA_a}\frac{(T_{fi}-T_a)}{G} \tag{20}$$

With the definitions in ISO 9806-1, the thermal efficiency of a solar collector is expressed as $\eta=\frac{\dot{m}c_f}{GA_a}(T_{fo}-T_{fi})$ and reduced temperature difference as $T^*=\frac{T_{fi}-T_a}{G}$. As a consequence, the thermal efficiency is given by

$$\eta=-\frac{\dot{m}c_f}{BGA_a}\left(\frac{d^2T_{fo}}{d\tau^2}+A\frac{dT_{fo}}{d\tau}-C\frac{dT_{fi}}{d\tau}\right)+\frac{E\dot{m}c_f}{BA_a}-\frac{F\dot{m}c_f}{BA_a}T^*. \tag{21}$$

On the assumption of ideal test conditions in the absolutely steady state, the inlet temperature is constant and the output temperature keeps constant as well since all other influencing factors including solar irradiance and heat loss of the collector do not change, thereby the

differential terms in Eq. (18) disappear. In addition, by setting $E\dot{m}c_f/BA_a = \eta_0$ and $F\dot{m}c_f/BA_a = a_1$, Eq. (21) is finally expressed as

$$\eta = \eta_0 - a_1 T^*. \tag{22}$$

Obviously, the deduction from Eqs. (17)–(22) proves that a close relationship between the new model and the first order model exists although they are suitable for two different test procedures.

2.3. Identification of model parameters

Both sides of Eq. (18) are divided by B and G_b so as to make the new model turn into the standardized form of multiple linear equation.

$$\frac{T_{fo}-T_{fi}}{G_b} = \frac{E_b}{B} - \frac{1}{BG_b}\frac{d^2T_{fo}}{d\tau^2} - \frac{A}{BG_b}\frac{dT_{fo}}{d\tau} + \frac{C}{BG_b}\frac{dT_{fi}}{d\tau} + \frac{E_dG_d}{BG_b} - F\frac{T_{fi}-T_a}{BG_b} \tag{23}$$

With the utilization of the basic numerical heat transfer method, the terms $dT_{fo}^2/d\tau^2$, $dT_{fo}/d\tau$, and $dT_{fi}/d\tau$ are treated with the averaged-difference method. By choosing N ($N > 3$) continuous recording points with the same time interval these differential terms become

$$\frac{d^2T_{fo}}{d\tau^2}(n) = \frac{T_{fo}(n+1)+T_{fo}(n-1)-2T_{fo}(n)}{\Delta\tau^2} \tag{24}$$

$$\frac{dT_{fo}}{d\tau}(n) = \frac{T_{fo}(n+1)-T_{fo}(n-1)}{2\Delta\tau} \tag{25}$$

$$\frac{dT_{fi}}{d\tau}(n) = \frac{T_{fi}(n+1)-T_{fi}(n-1)}{2\Delta\tau} \tag{26}$$

where $n = 2, \ldots, N-1$.

Consequently, with experimental data obtained from the dynamic test procedure presented just below, the model parameters in Eq. (23) will be identified by multiple linear regression tool.

3. Test procedure

In order to make a comparison between the steady state method and the dynamic one, the instrumentation and apparatus shown in Fig. 3 and Fig. 4 satisfy both the requirement of the steady state method mentioned in ASHRAE 93-2003 and the needs for dynamic method such as dramatic variation in the air temperature at the collector inlet.

3.1. Steady state test

According to the standard ASHRAE 93-2003, the instantaneous thermal efficiency of a solar collector was calculated as the ratio between the output power and the global solar irradiance as shown in Fig. 5. This standard requires a minimum of 16 data points at four different inlet temperatures to draw the thermal efficiency curve produced by using a least squares linear fit of the 16 data points.

For testing time constant of the solar air collector, after steady state conditions are achieved, the air collector is abruptly shielded from the sun light with an opaque cover. Then, the air temperatures at the inlet and outlet are continuously monitored as a function of time until

$$\frac{T_{fo,t}-T_{fi}}{T_{fo,initial}-T_{fi}} \langle 0.30. \tag{27}$$

Time constant is the time t required for the quantity $(T_{fo,t}-T_{fi})/(T_{fo,initial}-T_{fi})$ to change from 1.0 to 0.386. For the tested solar air collector, its time constant is 465 s as shown in Fig. 6.

3.2. Dynamic test

The dynamic test procedure was implemented to obtain the experiment data with two aims of the identification of model parameters and the comparison with results calculated from the regressed model. When the natural conditions did not cause fluctuations, the artificial adjustments were made to create some unsteady state conditions. For example, the inlet temperature varied sharply by controlling the electrical heater, and solar irradiance abruptly became nearly zero through shielding the collector from the solar radiation. During all tests, the data were acquired on 10-s intervals to capture transient conditions.

In case 1, as shown in Fig. 7 and Fig. 8, among this set of experimental data, there are five distinct periods categorized according to their impacts on testing the solar air collector. At the beginning, 10:30–10:57, it is suitable to perform the steady state test in the light of ASHRAE 93-2003. Unfortunately, from 10:58, albeit the global solar irradiance was at high value, all above 790 W/m^2, the diffuse solar irradiance was greater than 20% of global solar irradiance, hence, the steady state conditions did not exit any more. Then, 11:48–12:13, as the electrical heater was shut down, a sharp decrement in inlet temperature took place when the diffuse solar irradiance still constituted a relatively large percentage of the global solar irradiance. During the period from 12:14 to 13:17, the inlet temperature was kept nearly constant again. At the last period, 13:18–13:38, both of global solar irradiance and diffuse solar irradiance turned down expeditiously until G_d/G was close to 47%. In addition, the mass flow rate was ensured to be constant according to ASHRAE 93-2003 as shown in Fig. 9 by adjusting control valves. With these measured data and the method to identify model parameters described above, Eq. (23) is regressed to

$$T_{fo}-T_{fi} = 0.027G_b - 1.507\frac{d^2T_{fo}}{d\tau^2} - 0.476\frac{dT_{fo}}{d\tau} + 2.561\frac{dT_{fi}}{d\tau} + 0.033G_d - 0.024(T_{fi}-T_a) \tag{28}$$

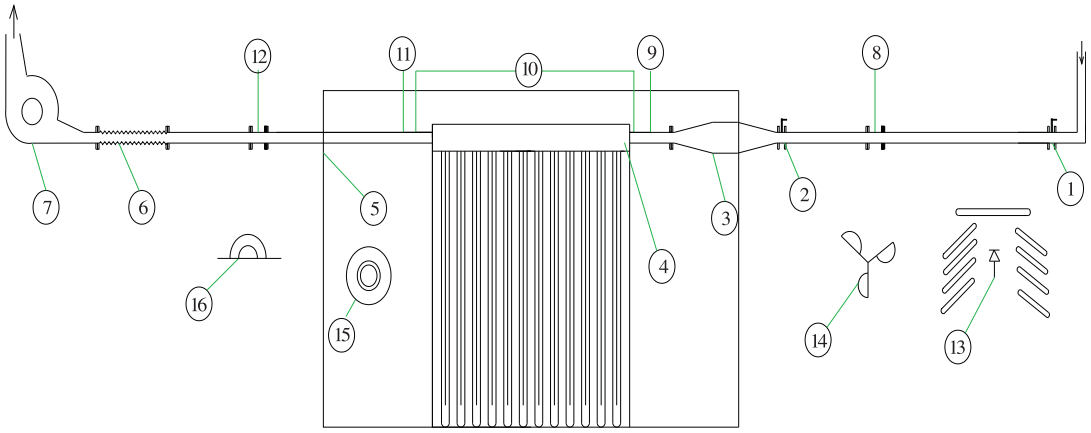

1. Control valve
2. Control valve
3. Electrical heater
4. Solar air collector
5. Rotating racket
6. Soft steel pipe
7. Induced draft fan
8. Turbine air flow meter
9. Inlet temperature sensor
10. Differential pressure measuring device
11. Outlet temperature sensor
12. Vortex air flow meter
13. Ambient temperature sensor
14. Wind velocity sensor
15. Pyranometer
16. pyrgeometer

Fig. 3. Schematic diagram of experimental set-up.

Fig. 4. Test facility of the solar air collector.

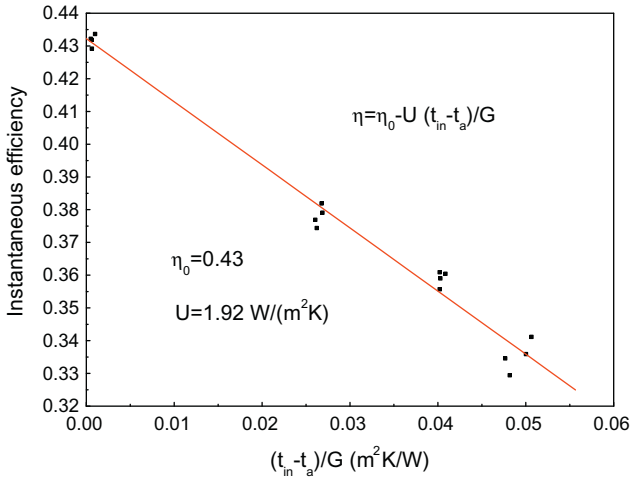

Fig. 5. Thermal efficiency curve of the solar air collector.

Case 2, as shown in Fig. 10, Fig. 11 and Fig. 12, is used for the comparison between the measured data and the predicted ones calculated with Eq. (28). In reality, so perfect were the weather conditions in Case 2 for the steady state test in ASHRAE 93-2003, and also the mass flowrate of the air through the collector was controlled at one value within the variation of ±2% during the whole period from 11:42 to 13:30. However, at the time 13:10, the electrical heater was turned off immediately in order to produce the transient data in relation to the variation in inlet temperature.

Figs. 13–15 show the case 3, also applied to the comparison, is composed of several diverse periods. Different from both cases 1 and 2, the mass flow rate was no more constant since there was no manual control on it. The relation between mass flow rate and the temperature, as shown in Figs. 14 and 15, illustrates that the approximately ten percent deviation of mass flow rate from the initial value was coincident with the variation in inlet tem-

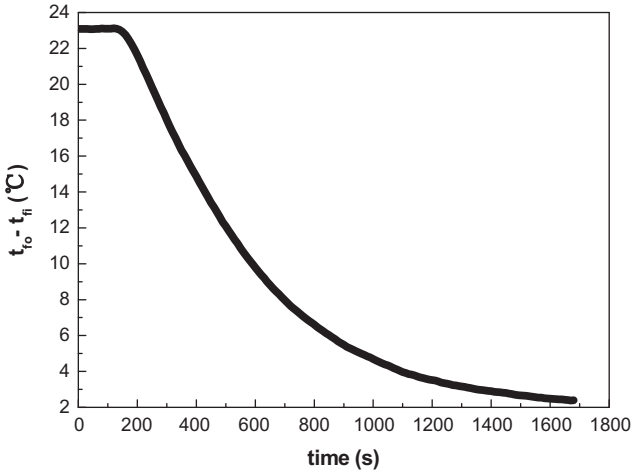

Fig. 6. Time constant of the solar air collector.

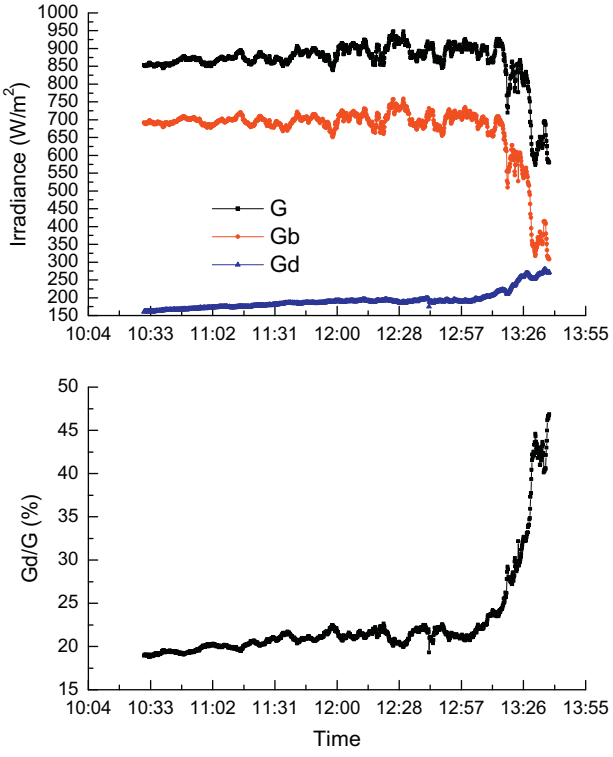

Fig. 7. Measured data for solar irradiance in Case 1.

perature mainly because the density of the heated air from about 15 °C to 45 °C decreased and the power of induced draft fan maintained almost constant. To start with, 10:40–12:03, it was a steady state condition in view of ASHRAE 93-2003. In the subsequent period, through turning on the electrical heater a severe rise in inlet temperature was followed with a relatively constant inlet temperature until the electrical heater was closed at 14:09, causing that a swift reduction in inlet temperature commenced. During the period from 14:11 to the end, three step changes in solar irradiance happened, with the result that both G_d and G equaled to near zero and the consequent G_d/G was near 100% when the solar air collector was suddenly shaded with an opaque cover.

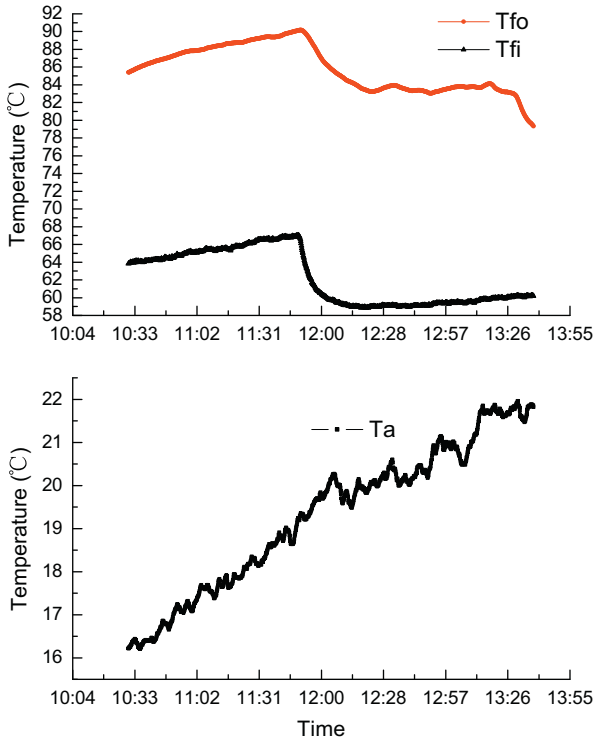

Fig. 8. Measured data for ambient, inlet and outlet temperatures in Case 1.

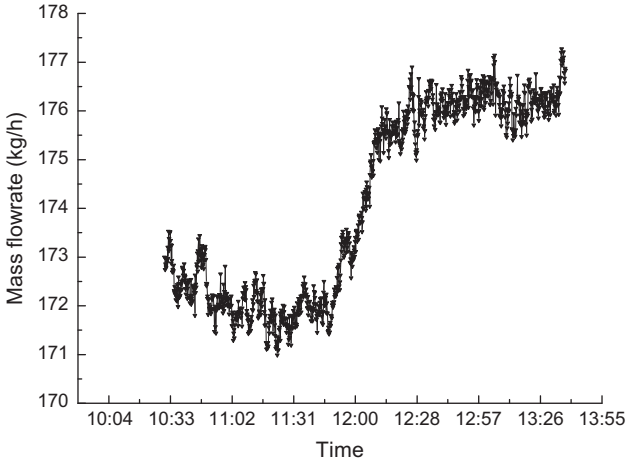

Fig. 9. Measured mass flow rate of the air through the solar collector in Case 1.

4. Results and discussion

The collector parameters obtained from test procedure Case 1 were presented in Eq. (28). As a consequence, the calculation of the outlet temperature of the collector was done according to the inlet temperature, ambient tempera-

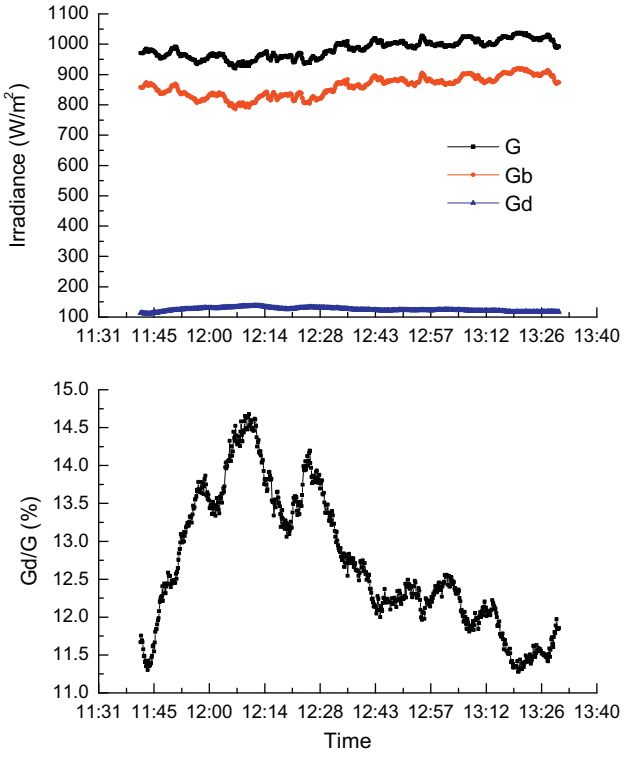

Fig. 10. Measured data for solar irradiance in Case 2.

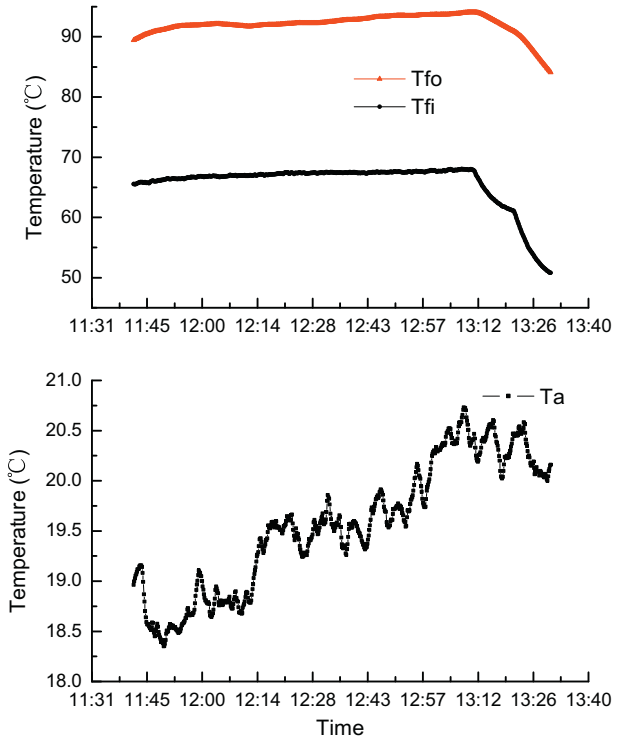

Fig. 11. Measured data for ambient, inlet and outlet temperatures in Case 2.

ture, and solar irradiance. Subsequently, the output energy and the thermal efficiency of the collector throughout the

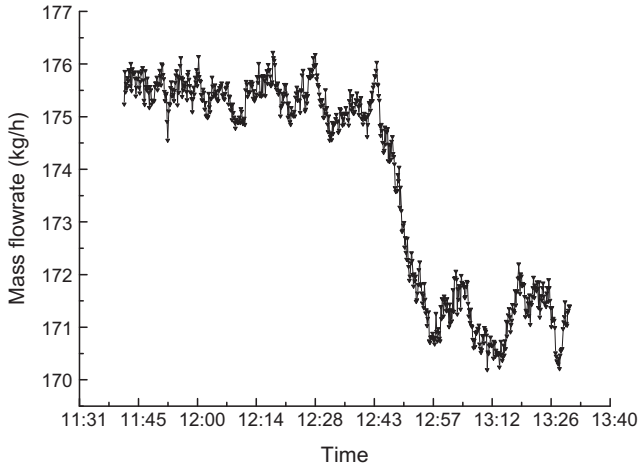

Fig. 12. Measured mass flow rate of the air through the solar collector in Case 2.

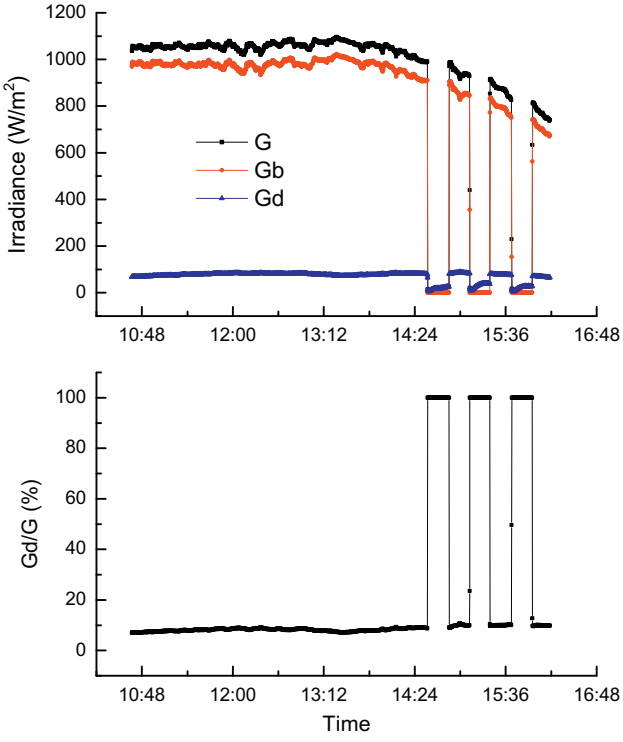

Fig. 13. Measured data for solar irradiance in Case 3.

test period were computed with the predicted outlet temperature.

The iterative technique was employed to calculate the predicted outlet temperature in order to get the differential terms in Eq. (28) according to Eqs. (24)–(26), which means this process continued until the solution converged. These calculated data needed to be smoothed for a better result. It was found that the measured outlet temperature lagged behind the predicted one in Fig. 16a(1). From the peak of predicted data to that of the measured one, the time was 460 s, which was quite close to the time tested constant

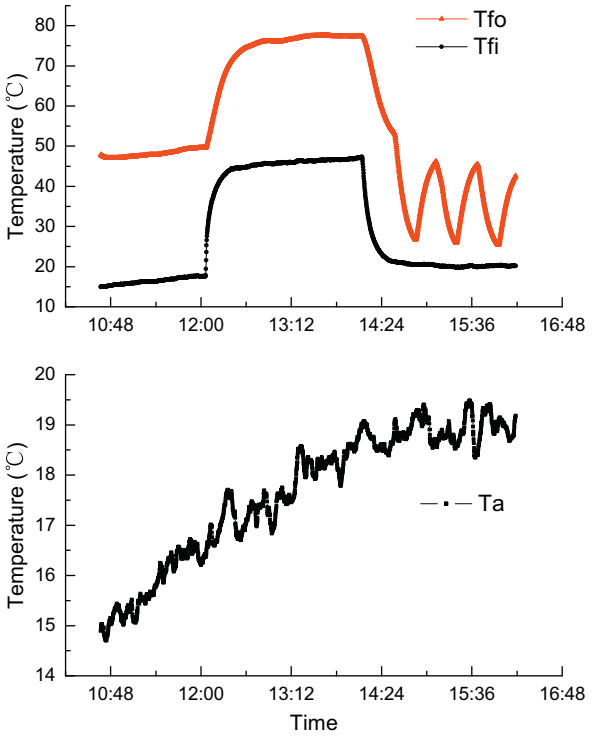

Fig. 14. Measured data for ambient, inlet and outlet temperatures in Case 3.

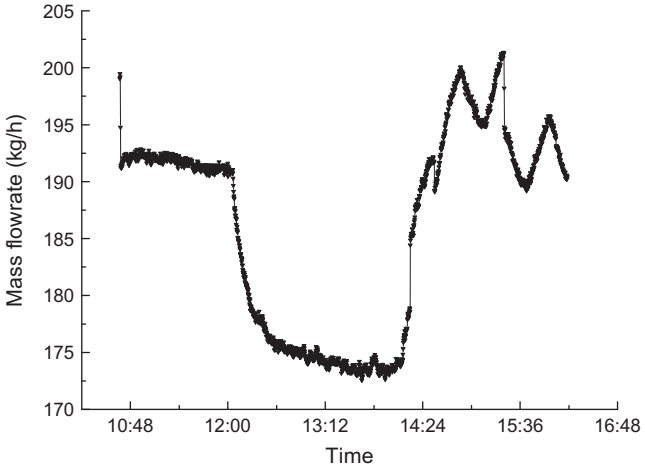

Fig. 15. Measured mass flow rate of the air through the solar collector in Case 3.

according to ASHRAE 93-2003 as shown in Fig. 6, hence this gave a new way to understand the time constant of a solar collector. Moreover, when the whole predicted data were moved backwards, namely a time-constant delay on predicted outlet temperature, the two lines in Fig. 16a(2) almost coincided with each other.

In the light of the method of calculation detailed above, Cases 2 and 3 were treated to obtain the outlet temperature as shown in Fig. 16b and c respectively. Accordingly, the results from calculations of predicted and measured data

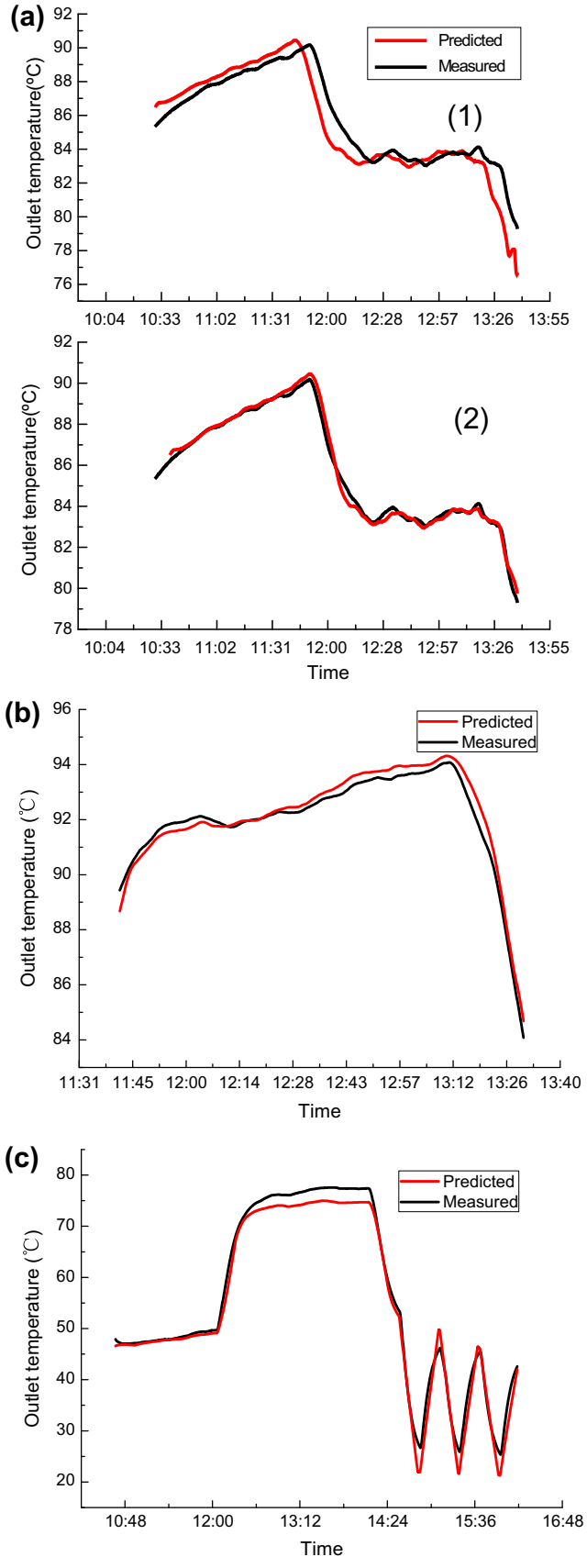

Fig. 16. Comparison between predicted and measured outlet temperatures (a) Case 1, (b) Case 2 and (c) Case 3.

Table 1
Comparison between predicted and measured calculations.

Case	Test time (HH:MM)	Predicted output energy (kJ)	Measured output energy (kJ)	Solar energy (kJ)	Predicted efficiency (%)	Measured efficiency (%)	Error (%)
1	10:30–13:38	12,499	12,485	34,695	36.03	35.98	0.05
2	11:42–13:30	8352	8304	23,867	34.99	34.79	0.20
3	10:40–16:10	25,651	27,193	64,342	39.87	42.26	2.39

were listed in Table 1. It proved that the dynamic method gave the accurate and reliable prediction for thermal performance of the solar air collectors. Although the result in Case 3 was not as good as the case 2 due to unsteady mass flow rate during the whole test period, however, it showed that this method gave the approximate outcome enough to be applied to engineering projects.

5. Conclusions

A detailed study on the new dynamic method for testing thermal performance of solar air collectors based on the basic theoretical knowledge of energy balance and the experimental procedures. Through the mathematical deduction, the dynamic model was proved to have a close relationship with the first order model in recognized standards. Only simple mathematical tools such as MLR, iteration, and smooth were employed to predict outlet temperature, output energy and thermal efficiency of solar air collectors by means of measured data obtained readily. Without increasing any new measurement parameter, the new method was suitable for the varying climate conditions. In comparison with the measured data and their calculating results, the minor errors, no more than 2.39%, mean that this method is reasonable and reliable. In addition, another way to obtain the time constant was offered through the same test procedure.

Consequently, less restriction in the test requirements suggests this method offers more convenient and cheaper tests, especially for places under unfavorable weather conditions. Additionally, this method is helpful for the designers to find out the output energy and thermal efficiency of solar air collectors according to the weather recourse.

Acknowledgment

This work has been supported by the National Natural Science Foundation of China (No. 51106150) and International S&T Cooperation Program of China (Grant No. S2012ZR0139). Especially, we would like to thank Li Xu's Master Supervisor Prof. Haigeng Chen at Northeastern University, Shenyang, China for his positive guidance.

References

Amer, E.H., Nayak, J.K., et al., 1999. A new dynamic method for testing solar flat-plate collectors under variable weather. Energy Conversion and Management 40 (8), 803–823.

ASHRAE 93-2003, 2003. Methods of Testing to Determine the Thermal Performance of Solar Collectors.

Budihardjo, I., Morrison, G.L., 2009. Performance of water-in-glass evacuated tube solar water heaters. Solar Energy 83 (1), 49–56.

EN 12975-1, 2006. Thermal Solar Systems and Components – Solar Collectors – Part 1: General Requirements.

Fischer, S., Heidemann, W., et al., 2004. Collector test method under quasi-dynamic conditions according to the European Standard EN 12975-2. Solar Energy 76 (1), 117–123.

Hou, H., 2005. Research on Dynamic Thermal Performance test Method of Solar Collectors. PH.D. Thesis, Shanghai Jiao Tong University, Shanghai, China.

Hou, H.J., Wang, Z.F., et al., 2005. A new method for the measurement of solar collector time constant. Renewable Energy 30 (6), 855–865.

ISO 9806-1, 1994. Test Methods for Solar Collectors – Part 1: Thermal Performance of Glazed Liquid Heating Collectors Including Pressure Drop.

Kratzenberg, M.G., Beyer, H.G., et al., 2006. Uncertainty calculation applied to different regression methods in the quasi-dynamic collector test. Solar Energy 80 (11), 1453–1462.

Liang, R.B., Ma, L.D., et al., 2011. Theoretical and experimental investigation of the filled-type evacuated tube solar collector with U tube. Solar Energy 85 (9), 1735–1744.

Ma, L.D., Lu, Z., et al., 2010. Thermal performance analysis of the glass evacuated tube solar collector with U-tube. Building and Environment 45 (9), 1959–1967.

Nayak, J.K., Amer, E.H., 2000. Experimental and theoretical evaluation of dynamic test procedures for solar flat-plate collectors. Solar Energy 69 (5), 377–401.

Tang, R., Yang, Y., et al., 2011. Comparative studies on thermal performance of water-in-glass evacuated tube solar water heaters with different collector tilt-angles. Solar Energy 85 (7), 1381–1389.

Zambolin, E., Del Col, D., 2010. Experimental analysis of thermal performance of flat plate and evacuated tube solar collectors in stationary standard and daily conditions. Solar Energy 84 (8), 1382–1396.